PNAS
www.pnas.org

Supplementary Information for

A hepatitis B virus causes chronic infections in equids worldwide

Andrea Rasche*, Felix Lehmann*, Nora Goldmann, Michael Nagel, Andres Moreira-Soto, Daniel Nobach, Ianei de Oliveira Carneiro, Nikolaus Osterrieder, Alex D. Greenwood, Eike Steinmann, Alexander N. Lukashev, Gerhard Schuler, Dieter Glebe, Jan Felix Drexler, and the Equid HBV Consortium

Jan Felix Drexler
Email: felix.drexler@charite.de

This PDF file includes:

Contents

Equid HBV Consortium (alphabetical order)

Alvaro Aguilar-Setien: Mexican Social Security Institute (IMSS), Medical Immunology Research Unit, National Medical Center Siglo XXL, Mexico City, Mexico

Walid Azab: Freie Universität Berlin, Institute für Virologie, Berlin, Germany

Augusto Carluccio: Università degli Studi di Teramo, Faculty of Veterinary Medicine, Teramo, Italy

Dimo Dietrich: Department of Otolaryngology, Head and Neck Surgery, University Hospital Bonn, Bonn, Germany

Carlos Roberto Franke: Federal University of Bahia, Salvador, Brazil

Ignacio García-Bocanegra: Universidad de Córdoba, Córdoba, Spain

Fernando García-Lacy: PhD program of Production and Animal Health Sciences, National Autonomous University of Mexico, Faculty of Veterinary Medicine and Zootechnics, Mexico City, Mexico

Lara M. Jeworoski: Institute of Virology, Charité-Universitätsmedizin Berlin, corporate member of Freie Universität Berlin and Humboldt-Universität zu Berlin, Berlin, Germany

Jörg Jores: International Livestock Research Institute, Nairobi, Kenya; University of Bern, Institute of Veterinary Bacteriology, Bern, Switzerland

Ramona Kepper: Justus Liebig University, Institute of Medical Virology, National Reference Center for Hepatitis B Viruses and Hepatitis D Viruses, Giessen, Germany; German Centre for Infection Research (DZIF), Germany

Eduardo Martins Netto: Federal University of Bahia, Salvador, Brazil

Ellis Owusu-Dabo: Kwame Nkrumah University of Science and Technology, School of Public Health, Kumasi, Ghana

Jorge R.L. Ribas: Bahia State Agricultural Defense Agency, Salvador, Brazil

Christina Roncoroni: Istituto Zooprofilattico Sperimentale Lazio e Toscana, Rome, Italy

Pia L. Roppert: Justus Liebig University, Institute of Medical Virology, National Reference Center for Hepatitis B Viruses and Hepatitis D Viruses, Giessen, Germany; German Centre for Infection Research (DZIF), Germany

Anton Rusenov: Trakia University, Faculty of Veterinary Medicine, Department of Internal Diseases, Stara Zagora, Bulgaria

Nikolina Rusenova: Trakia University, Stara Zagora, Faculty of Veterinary Medicine, Department of Veterinary Microbiology, Infectious and Parasitic Diseases, Bulgaria

Nikolay Sandev: Trakia University, Stara Zagora, Faculty of Veterinary Medicine, Department of Veterinary Microbiology, Infectious and Parasitic Diseases, Bulgaria

Peter A. Seeber: Leibniz Institute for Zoo and Wildlife Research, Berlin, Germany; Limnological Institute, University of Konstanz, Germany

Anat Shnaiderman-Torban: Koret School of Veterinary Medicine, The Robert H. Smith Faculty of Agriculture, Food and Environment, The Hebrew University of Jerusalem, Rehovot, Israel

Amir Steinman: Koret School of Veterinary Medicine, The Robert H. Smith Faculty of Agriculture, Food and Environment, The Hebrew University of Jerusalem, Rehovot, Israel

Birthe Tegtmeyer: Institute for Experimental Virology, TWINCORE Centre for Experimental and Clinical Infection Research, Medical School Hannover (MHH) – Helmholtz Centre for Infection Research (HZI), Hannover, Germany

Vincenzo Veneziano: University of Naples Federico II, Department of Veterinary Medicine and Animal Productions, Naples, Italy

Maria C. Veronesi: Università degli Studi di Milano, Department of Veterinary Medicine, Milan, Italy

Stephanie Walter: Institute for Experimental Virology, TWINCORE Centre for Experimental and Clinical Infection Research, Medical School Hannover (MHH) – Helmholtz Centre for Infection Research (HZI), Hannover, Germany

Dimitrinka Zapryanova: Trakia University, Faculty of Veterinary Medicine, Department of Pharmacology, Veterinary Physiology, and Physiological Chemistry, Stara Zagora, Bulgaria

Contributions

DD, LMJ, RK, PLR, BT, SW: performed research

AAS, WA, AC, IGB, FGL, JJ, EMN, EOD, JRLR, CRF, CR, AR, NR, NS, PS, AST, AS, VV, MCV, DZ: contributed new reagents/analytical tools

Supplementary Methods

Sampling

A total of 793 serum specimens were collected from domestic donkeys during 2007-2016 in Germany, Bulgaria, France, Spain, Italy, Israel, Kenya, Costa Rica, and Mexico, and 53 serum samples were collected from Bulgarian mules (1). Organ and serum specimens from 84 donkeys were collected from abattoirs in northern Ghana in 2015. A total of 29 serum specimens form zebras (*Equus quagga* and

Equus zebra) were collected from 2015-2016 in Tanzania (Commission for Science and Technology permit No. 2015-168-NA-90-130) and Namibia (Ministry of Environment and Tourism permit No. 2094/2016). Longitudinal sampling of German donkeys was conducted during 2007-2008 as described previously (2). Serum specimens from domestic horses (*Equus caballus*) were sampled in Brazil from 2013-2018 (1,170 specimens, permit ID MAPA 001/18; CEUA 55/2017), Spain (607 specimens, permit ID BOJA55-20/2012) and Germany (181 specimens, collected for diagnostic purposes during veterinary treatment).

DNA purification, virus detection and quantification, and complete genome amplification

For DNA purification approximately 30 mg of tissue were extracted using the MagNA Pure 96 DNA and Viral NA large-volume kit (Roche, Penzberg, Germany). Twenty microliters of serum were extracted using the MagNA Pure DNA and Viral NA small-volume kit (Roche). Hepadnavirus DNA detection was performed using a broadly reactive hemi-nested PCR assay as described (3). Viral loads were determined using the following strain specific real-time assay (5'-3'): Forward primer, CAA AGT GCC TTG GCC AAA AT; Probe, FAM-TGC CGT ACC CAA CCT GCG ATC ACT-BHQ1; Reverse primer, CAA GTC ACA GGA CAR GAT GTT GGT. Quantification was performed using photometrically quantified plasmid standards containing the PCR target region cloned into pCR4-TOPO TA vectors (Thermo Fisher Scientific, Waltham, USA). Thermocycling was conducted as described previously (3). Complete genomes were amplified using a strain-specific nested PCR with primers binding close to the 5' and 3' ends of the screening fragment. Oligonucleotide sequences were (5'-3'): Forward primer, CTT CGG ACA GCA ACT GCA C; Forward nested primer, CAT CAT GGG CTT TCG GAA G; Reverse primer, CAC ATC CAG CGA TAA CCA GTA C; Reverse nested primer, GAG TGA TCG CAG GTT GGG TAC. If complete genome sequencing was unsuccessful, smaller fragments were amplified using strain-specific assays.

EqHCV RNA was detected using a strain specific real-time assay as published (4).

High-throughput sequencing

High-throughput sequencing (HTS) and single nucleotide polymorphism (SNP) analyses were done as described (5). In short, library preparation and Illumina MiSeq sequencing were performed using KAPA Frag Kit, KAPA HyperPrep kit (Roche Molecular Diagnostics, Basel, Switzerland), and MiSeq reagent v2 chemistry (Illumina San Diego, USA). SNP analysis was performed using trimmed and mapped reads against EqHBV genomes in Geneious 9.1.8 (6). Only SNPs occurring in >2.5% of at least 200 reads were considered.

Evolutionary analyses

Sequences were aligned using the MAFFT package (7) in Geneious 9.1.8 (6). Gaps and ambiguous sequence positions were removed from the alignments. Maximum likelihood phylogenetic trees were built in MEGA7 (8) using a Hasegawa-Kishino-Yano (HKY) substitution model and 1,000 bootstrap replicates. Bayesian phylogenies were calculated in MrBayes V3.1 (9). Patristic distances were calculated in MEGA7. Ancestral state reconstructions (ASR) and hypothesis testing were conducted in BEAST V1.10 (10) as described (11) using a HKY+G substitution model and a Yule speciation process tree prior. Trees were midpoint-rooted, annotated using a burn-in of 25% in TreeAnnotator, and were visualized using FigTree (10). For ASR, only EqHBV sequences were analyzed under a strict clock. For TMRCA calculation and hypothesis testing, an uncorrelated relaxed clock was used, with a mean rate of $1x10^{-5}$ calibrated according to Muhlemann et al., 2018 (12). Hypothesis testing was conducted with an alignment including all hepadnavirus species from Laurasiatherian hosts. According to Rasche et al. (13), the MRCA of the root was calibrated with the origin of Laurasiatheria of 80.5 million years ago (mya), 95% Highest Posterior Density (HPD), 79.7-81.3 (14). In addition, EqHBV MRCAs of viruses originating from two donkey populations were calibrated according to estimates based on tip-dating. These included all donkeys from Germany using a normally distributed prior, 97.8 years ago (ya), 95% HPD, 35.9-195.6, and a second prior describing the origin of all EqHBV sequences from Ghanaian donkeys (normally distributed prior, 691.1 ya, 95% HPD, 354-1,183.2). The root of all Laurasiatherian hepadnaviruses was calibrated using normally distributed priors describing different time points in evolution, domestication, and distribution of donkeys as shown in **Fig. 5D**, including the origin of the genus *Equus* (4.1 mya, 95% HPD, 4.0-4.5) (15), the origin of the clade comprising donkeys and zebras (2.9 mya, 95% HPD, 2.8-3.1) (16), the domestication of donkeys (5-6 kya) (17) (mean, 5,500; standard deviation, 300), and the worldwide dispersal of domesticated donkeys with the arrival of Christopher Columbus in the Americas (18), approximately 500 ya (mean, 500; standard deviation, 20). Marginal likelihoods estimation (MLE) was used to evaluate which of the four priors best described the root of EqHBV in our dataset. MLE was performed using the path sampling/stepping-stone algorithm with 100 path steps and chain lengths of 1,000,000 generations (19).

Genomic analyses

Similarity plots were generated in SSE (20), using a window size of 300 nucleotides and a step size of 100 nucleotides. Bootscan analyses were done with SimPlot 3.5.1 (21), using a window size of 450 nucleotides and a step size of 20 nucleotides for equid strains only and a window size of 300 nucleotides and a step size of 20 nucleotides for EqHBV and reference hepadnaviruses.

Antibody detection

Detection of antibodies against HBV proteins was performed using an immunofluorescence assay as described before (3). For antibody screening, HuH7 cells were transfected with a 1.1 overlength expression plasmid of HBV (for antibody screening) as described (3) or a pcDNA3.1+ plasmid encoding the core protein of HBV subgenotype D3 (for longitudinally sampled German donkeys). Cells were fixed and permeabilized, incubated for 1.5-2 h at 37°C with serum samples diluted (1:40 for antibody screening and serially diluted as described below for longitudinally sampled German donkeys) in Euroimmun sample buffer (Euroimmun, Lübeck, Germany) and washed three times with PBS containing 0.1 % Tween (PBS-T). Cells were then incubated with a 1:500 dilution of the secondary antibody (rabbit anti-donkey IgG, Bethyl, Montgomery, US) for 1 h at 37°C, washed 3 times with PBS-T, and incubated with a 1:400 dilution of a Cy3-labeled goat anti-rabbit antibody (Jackson Immuno Research, West Grove, USA) for 30 min at 37°C. After washing three times with PBS-T, cells were rinsed once in water. Dried cells were mounted with DAPI Gold Mounting Medium (Thermo Fisher Scientific). An antiserum against human HBc produced in rabbit (Eurogentec, Liège, Belgium) was used as a positive control. Co-staining was conducted by co-incubating of the secondary antibody and sheep anti-HBc serum (1:2000) and co-incubating of the third antibody with donkey anti-sheep Alexa Fluor® 488 labeled antibody (1:200) (Jackson Immuno Research). Antibodies against EqHCV were detected using a luciferase immunoprecipitation system as described (1) for sera samples from Ghanaian donkeys and Tanzanian zebras. All other EqHCV seroprevalence rates given in **Fig. 1 E-G** were published before (1).

In vitro infection experiments

HDV pseudotyped with surface proteins of EqHBV (Italian donkey strain Do-86), EqHBV (zebra strain S2581) and HBV were produced as described previously (5), using equimolar amounts of expression plasmids encoding a trimer of the human HDV genome and expression plasmids encoding hepadnavirus L-ORFs transfected into HuH7 cells. Secretion of HDV was quantified by quantitative reverse transcription PCR (RT-qPCR). Infection experiments were performed with i) transiently transfected HepG2 cells or ii) cryopreserved primary hepatocytes. i) HepG2 cells were transfected with human sodium (Na+) taurocholate cotransporting polypeptide (NTCP)- or donkey Ntcp-encoding plasmids under CMV promoter as described before (5). A taurocholate transport assay was performed using NBD-TC (fluorescent bile acid 4-nitro-2,1,3-benzoxadiazole taurocholic acid) as published (5), to assess the physiological functionality of the NTCP/Ntcp. ii) Cryopreserved primary equine hepatocytes (PEH) derived from horses or primary human hepatocytes (PHH) (Primacyt, Schwerin, Germany) were thawed and plated on collagenized 24-well plates according to manufacturer's instruction. After overnight attachment of cells, a taurocholate transport assay was performed as described above. PEHs were also fixed, permeabilized, blocked as described (5) and stained for the equid NTCP orthologue using a 1:50

dilution of a cross-reactive NTCP-antibody (HPA-042727 (Sigma-Aldrich, Darmstadt, Germany) and a 1:400 dilution of anti-rabbit-IgG antibody coupled to Alexa-488 (Invitrogen, Karlsruhe, Germany).

On the same day as the NBD-TC assay, cells were infected with equimolar amounts of either HDV_{HBV}, $HDV_{EqHBV\text{-}donkey}$ or $HDV_{EqHBV\text{-}zebra}$ ($1x10^8$ copies per well). PEHs were also infected with HBV ($1.5x10^5$ copies/well) produced using a 1.1mer HBV overlength construct of subgenotype D3 (3) as well as EqHBV-positive sera ($6.8x10^5$-$1.0x10^6$ copies/well). Inhibition of HBV infection by specific antibodies was performed by pre-incubation with a serum of a rabbit immunized with a human HBV-vaccine or an EqHBV-antibody positive donkey serum. Medium was changed every day until day 11, when cells were fixed for the immunofluorescence assay (IFA). Cell culture supernatant was collected every second day and stored at -20°C. IFA was performed on permeabilized cells as described (5) using human anti-HDV-positive serum and anti-human-IgG antibody coupled to Alexa-568 (Invitrogen, Karlsruhe, Germany). Nuclei were stained with DAPI (Thermo Fisher Scientific). For measurement of HBeAg, 150 µl inoculum and cell culture supernatants of EqHBV/HBV infected cells day 3 to day 11 post infection were tested in a commercial HBeAg assay (Abbott, Chicago, USA).

Cloning of 1.5mer overlength plasmids and transfection experiments

EqHBV sequences of Do-86 and S2581 were cloned as 1.5mer overlength constructs into pcDNA3.1+ via recombination as described previously (5).

HepG2 cells were transfected as described above with the 1.5mer overlength plasmids. Medium was changed to William's Medium E without phenol red (Thermo Fisher Scientific, Waltham, USA) supplemented with 2% FCS and 2mM glutamine on day 1 post transfection (p.t.) and exchanged again on day 3. Supernatant was collected on day 5 p.t. and HBeAg was measured as described above. Once supernatant was removed, cells were prepared for immunofluorescence analysis as described above and stained with a 1:100 dilution of a cross-reactive anti-WHV-HBc polyclonal rabbit serum (kindly provided by R. G. Ulrich) and a 1:400 dilution of anti-rabbit-IgG antibody coupled to Alexa-594 (Invitrogen, Karlsruhe, Germany).

Longitudinally studied donkeys

Longitudinal samples were acquired in a previous study (2). First and last samples of all individuals (n= 45, 9 males, 36 females) were tested for antibodies against EqHBV and EqHCV, and for EqHBV DNA and EqHCV RNA as described above. Monthly sampled specimens were tested of those positive for either antibodies or DNA in at least one time point. For antibody detection, serial dilutions (1:40, 1:400, 1:4,000) were tested using HuH7 cells transfected with an expression plasmid containing HBc (described above). HTS of all PCR-positive samples was conducted as described above. Mutations impeding the translation of HBe were excluded by SNP analyses of the preC/Core encoding region using HTS data. As detailed above, SNP occurring in >2.5% of at least 200 reads were considered. Co-

infection with EqHCV was excluded by specific RT-qPCR and testing against antibodies as described. Measurement of liver parameters was conducted by Laboklin, Bad Kissingen, Germany. Selected liver parameters typically used as indicators for liver damage in equids including alkaline phosphatase, aspartate aminotransferase, and gamma-glutamyltransferase (22) were depicted.

Liver inflammation and fibrosis

A total of 49 histological sections of formalin-fixed paraffin-embedded liver specimens from Ghanaian donkeys was used to evaluate liver inflammation and fibrosis. All liver samples were tested for EqHBV DNA and EqHCV RNA as described above. EqHBV and EqHCV antibody detection was performed as described above of those animals, for which sera was available (n=25) (**Supplementary Table S3**). Liver inflammation was evaluated using hematoxylin and eosin stain (HE stain) of sections and graded by Batts-Ludwig scoring as described (23). Evaluation of fibrosis of the livers was performed using Picrosirius Red-stained sections (24). For this, sections were rehydrated, and nuclei were stained with Weigert's hematoxylin (Carl Roth, Karlruhe, Germany). Next, sections were washed once in water and stained for one hour in Picrosirius Red-solution (0.1 g Sirius Red in 100 mL saturated picric acid solution) (Sigma-Aldrich, Munich, Germany). Afterwards, they were washed twice in diluted acidic acid (10 mL acidic acid in 22 mL distilled water) (Carl Roth), dehydrated and mounted in xylene (Carl Roth). In stained sections, collagen representing fibrosis appears red. Fibrosis was graded into 7 stages according to Ishak score (25). Ishak 0, no signs of fibrosis; Ishak 1, mild fibrosis recognizable by fibrous expansion on some portals; Ishak 2, mild fibrosis recognizable by fibrous expansion on most portals; Ishak 3, moderate fibrosis with fibrous expansion on most portals and some fibrous bridges between portal areas; Ishak 4, severe fibrosis with extensive fibrous expansion of portals and numerous fibrous bridges between portal areas; Ishak 5, incomplete cirrhosis with focal reorganization of the liver parenchyma with hepatocellular regeneration and degeneration together with fibrosis; Ishak 6, cirrhosis affecting the whole liver parenchyma.

For statistical analyses, all samples graded with a Batts-score of I or higher were grouped as positive for inflammation and Ishak level 3 or higher were considered fibrosis positive.

Statistical analyses

All statistical analyses were conducted in GraphPad Prism V7 (www.graphpad.com). Comparison of antibody detection rates and pathological analyses were performed using 2x2 contingency tables and two-tailed Fisher's exact test. To compare detection rates among age groups, we used chi-square tests for trends. To test for liver tropism, we compared viral concentrations in liver to mean viral concentrations in all other solid organs and blood using a two-tailed unpaired t-test.

Virus abbreviations

ASHV, arctic squirrel hepatitis virus; ChimpHBV, Chimpanzee HBV; CMHBV, capuchin monkey HBV; CSHBV, crowned shrew HBV; DCHBV, domestic cat HBV; GibHBV, Gibbon HBV; GorHBV, Gorilla HBV; GSHV, ground squirrel hepatitis virus; HBHBV, horseshoe bat HBV; LBHBV, long-fingered bat HBV; MDHBV, Maxwell's duiker HBV; MSHBV, musk shrew HBV; OrHBV, Orangutan HBV; PBHBV, pomona bat HBV; RBHBV, roundleaf bat HBV; TBHBV, tent-making bat HBV; WHV, woodchuck hepatitis virus; WMHBV, woolly monkey HBV;

Supplementary Figures and Tables

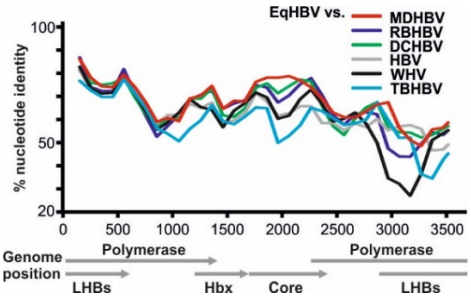

Fig. S1. Distance plot of EqHBV and reference viruses.

Percentage nucleotide identity of EqHBV compared to selected reference viruses. Window size 250 nt, step size 25 nt.

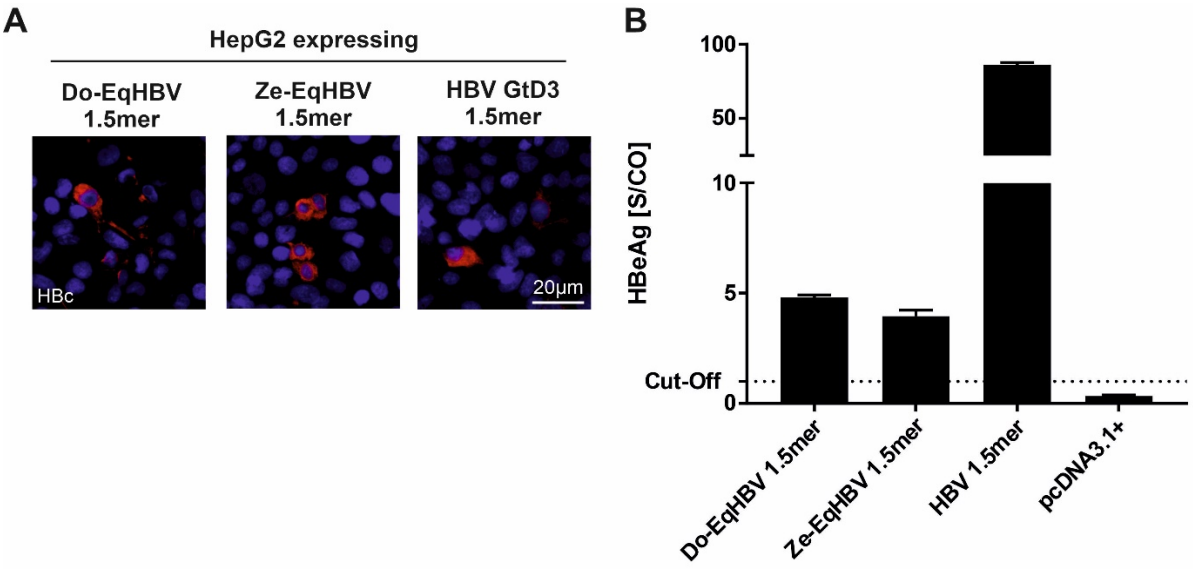

Fig. S2. Production of HBc and HBeAg of EqHBV expression constructs after transfection of HepG2 cells.

A) Immunofluorescence staining of intracellular HBc expression of HepG2 cells after transfection with 1.5mer overlength constructs encoding two distinct EqHBV strains (originating from donkey (Do-EqHBV) or zebra (Ze-EqHBV)) and HBV genotype D3 (GtD3). B) HBeAg production after transfection of HepG2 cells with EqHBV and HBV 1.5mer constructs using a commercial HBeAg detection kit (Architect, Abbott, Chicago, USA). N=2. S/CO, signal to cut-off ratio.

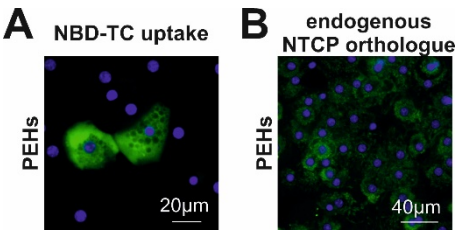

Fig. S3. Functional expression of equid NTCP orthologue in primary equid hepatocytes (PEH).

A) Taurocholate (NBD-TC) uptake (green) by PEHs. B) Immunofluorescence staining of equid NTCP orthologue in PEHs with a cross-reactive anti-NTCP antibody.

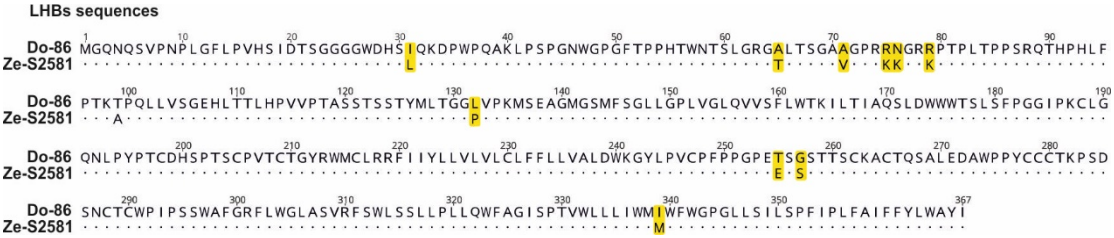

Fig. S4. EqHBV LHBs amino acid sequence alignment.

Alignment includes donkey (Do-86) and zebra (Ze-S2581) EqHBV sequences. Dots indicate identical amino acids; differences are highlighted in yellow.

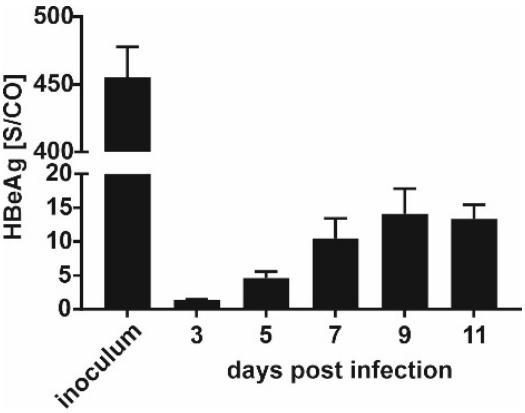

Fig. S5. Time-resolved HBeAg production after infection of primary equid hepatocytes (PEH) with HBV.

HBeAg production after infection of PEH with cell culture-derived HBV particles using a commercial HBeAg detection kit (Architect, Abbott, Chicago, USA). N=2. PEH, primary equine hepatocytes; S/CO, signal to cut-off ratio.

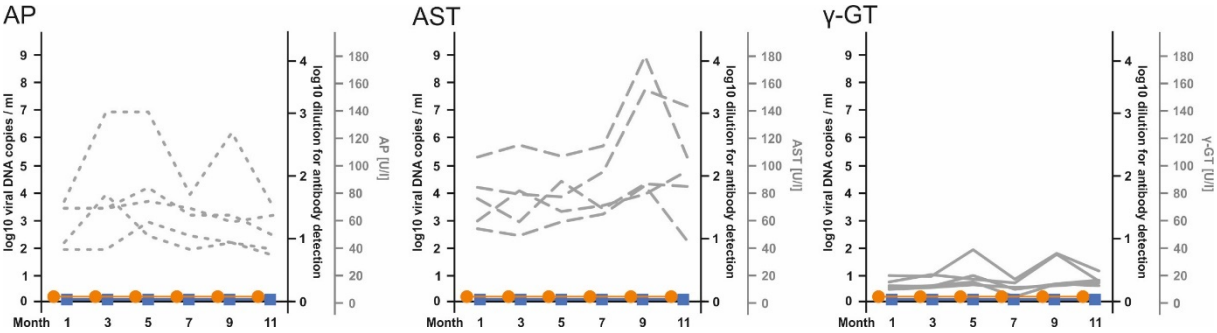

Fig. S6. Liver parameters of five EqHBV negative longitudinally sampled donkeys.

To compare concentrations of liver parameters in EqHBV positive (**Fig. 4**) to EqHBV negative animals, Alkaline phosphatase (AP), aspartate aminotransferase (AST) and gamma-glutamyl transferase (gamma-GT) were measured in longitudinal samples of five female donkeys (EqHBV DNA- and antibody-negative) from the same sample cohort.

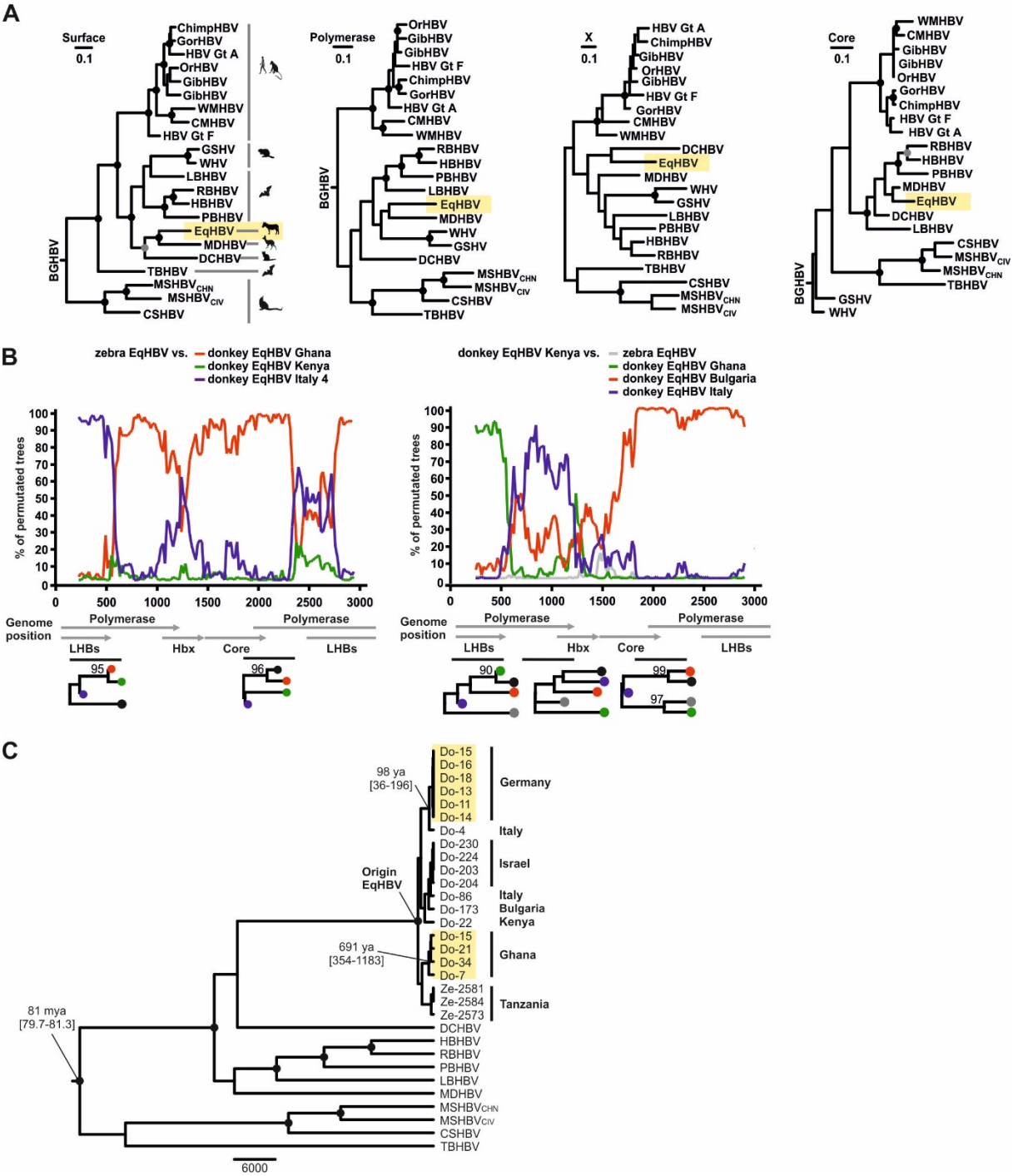

Fig. S7. Evolutionary reconstructions of EqHBV.

A) Orthohepadnavirus phylogenies of translated open reading frames (ORF). Bayesian phylogeny of translated surface, polymerase and core ORF, including EqHBV, reference hepadnaviruses and bluegill HBV (BGHBV) as an outgroup were calculated in MrBayes V3.1. An unrooted Maximum Likelihood (ML) phylogeny was used for the translated X ORF due to the lack of an outgroup. Filled circles indicate posterior probability >0.95 (black) and >0.90 (grey) for Bayesian phylogenies, and a bootstrap support of >85% (black) for ML phylogenies (1,000 bootstrap replicates). B) Bootscan graph of EqHBV strains. Window size of 300 nucleotides and a step size of 100 nucleotides. C) Midpoint rooted phylogenetic reconstruction of Laurasiatherian hepadnaviruses (complete genomes) used for hypothesis testing in BEAST. mya, million years ago; ya, years ago.

Table S1. Genomic sequence distances between EqHBV and hepadnavirus reference species.

Virus genus	Virus	Nucleotide distance to all EqHBV strains (%)
Orthohepadnavirus	MDHBV	30.4-31.1
	HBHBV	31.9-32.5
	LBHBV	32.1-33.0
	DCHBV	32.8-33.4
	RBHBV	32.9-33.4
	PBHBV	34.0-34.5
	GSHBV	36.0-36.5
	HBV	36.4-36.9
	CMHBV	36.5-37.1
	WHV	36.6-37.3
	WMHBV	36.9-37.4
	TBHBV	39.2-39.9
	CSHBV	41.9-42.4
	MSHBV	42.0-42.7
Avihepadnavirus	DHBV	58.1-58.6

Table S2. Sample characteristics of seropositive donkeys.

	Sex			Age (years)						
	male	**female**	**unknown**	**0-1**	**2-5**	**6-10**	**11-15**	**16-20**	**21-30**	**unknown**
EqHBV Ab positive	12	26	5	1	7	7	6	5	3	14
EqHBV Ab negative	235	481	60	75	140	185	90	69	35	182
Total (% seropositive)	**247 (4.9)**	**507 (5.1)**	**65 (7.7)**	**76 (1.3)**	**147 (4.8)**	**192 (3.6)**	**96 (6.3)**	**74 (6.8)**	**38 (7.9)**	**196 (7.1)**

Ab, Antibody

Table S3. Histopathological analyses of donkey liver specimens.

ID	EqHBV cp/g	EqHBV Ab	EqHCV	EqHCV Ab	Inflammation (Ludwig-Batts score)	Fibrosis (Ishak score)
Li-09	neg	n.d.	neg	n.d.	neg	1
Li-10	1,07E+05	n.d.	neg	n.d.	II	4
Li-11	neg	n.d.	neg	n.d.	neg	4
Li-12	neg	n.d.	neg	n.d.	neg	2
Li-13	neg	n.d.	neg	n.d.	neg	3
Li-14	neg	n.d.	neg	n.d.	neg	1
Li-15	1,11E+06	n.d.	neg	n.d.	I	4
Li-16	neg	n.d.	neg	n.d.	neg	1
Li-17	neg	n.d.	neg	n.d.	neg	2
Li-18	neg	n.d.	neg	n.d.	n.d.	4
Li-19	neg	n.d.	neg	n.d.	n.d.	3
Li-20	neg	n.d.	neg	n.d.	neg	2
Li-21	neg	n.d.	neg	n.d.	neg	1
Li-22	neg	n.d.	neg	n.d.	neg	3
Li-23	neg	n.d.	neg	n.d.	neg	1
Li-24	neg	n.d.	neg	n.d.	II	3
Li-25	neg	neg	neg	pos	n.d.	4
Li-26	neg	neg	neg	pos	neg	1
Li-27	neg	neg	neg	pos	neg	4
Li-28	neg	neg	neg	pos	n.d.	3
Li-29	neg	neg	neg	pos	neg	2
Li-30	neg	neg	neg	pos	neg	3
Li-31	neg	neg	neg	pos	neg	4
Li-32	neg	neg	neg	pos	neg	2
Li-33	neg	neg	neg	pos	n.d.	4
Li-34	1,96E+05	pos	neg	pos	I	3
Li-35	2,62E+06	pos	neg	pos	II	3
Li-36	neg	neg	neg	pos	I	4
Li-37	neg	neg	neg	pos	I	4
Li-38	neg	neg	neg	pos	n.d.	4
Li-39	neg	neg	neg	pos	n.d.	3
Li-40	neg	neg	neg	pos	neg	3
Li-41	2,04E+11	pos	neg	pos	neg	3
Li-42	neg	neg	neg	pos	n.d.	3
Li-43	1,07E+07	pos	neg	pos	I	4
Li-44	neg	neg	neg	pos	n.d.	4

Li-45	neg	neg	neg	pos	neg	2
Li-46	neg	neg	neg	pos	n.d.	4
Li-47	neg	neg	neg	pos	neg	4
Li-48	neg	neg	neg	pos	n.d.	3
Li-49	neg	pos	neg	pos	n.d.	3
Li-50	neg	n.d.	neg	n.d.	n.d.	2
UF-11	neg	n.d.	neg	n.d.	neg	2
UF-13	neg	n.d.	neg	n.d.	neg	3
UF-14	neg	n.d.	neg	n.d.	neg	3
UF-22	neg	n.d.	neg	n.d.	neg	2
UF-26	neg	n.d.	neg	n.d.	I	1
UF-35	neg	n.d.	neg	n.d.	n.d.	2
UF-38	neg	n.d.	neg	n.d.	neg	1

Ab, antibodies; n.d, no data

SI References

1. S. Walter *et al.*, Differential Infection Patterns and Recent Evolutionary Origins of Equine Hepaciviruses in Donkeys. *J Virol* **91** (2017).
2. B. Hoffmann, A. W. Bernhardt, K. Failing, G. Schuler, [Profiles of estrone, estrone sulfate and progesterone in donkey (Equus asinus) mares during pregnancy]. *Tierarztl Prax Ausg G Grosstiere Nutztiere* **42**, 32-39 (2014).
3. J. F. Drexler *et al.*, Bats carry pathogenic hepadnaviruses antigenically related to hepatitis B virus and capable of infecting human hepatocytes. *Proc Natl Acad Sci U S A* **110**, 16151-16156 (2013).
4. K. Schlottau, S. Fereidouni, M. Beer, B. Hoffmann, Molecular identification and characterization of nonprimate hepaciviruses in equines. *Arch Virol* **164**, 391-400 (2019).
5. A. Rasche *et al.*, Highly diversified shrew hepatitis B viruses corroborate ancient origins and divergent infection patterns of mammalian hepadnaviruses. *Proc Natl Acad Sci U S A* 10.1073/pnas.1908072116 (2019).
6. M. Kearse *et al.*, Geneious Basic: an integrated and extendable desktop software platform for the organization and analysis of sequence data. *Bioinformatics* **28**, 1647-1649 (2012).
7. K. Katoh, K. Misawa, K. Kuma, T. Miyata, MAFFT: a novel method for rapid multiple sequence alignment based on fast Fourier transform. *Nucleic Acids Res* **30**, 3059-3066 (2002).
8. S. Kumar, G. Stecher, K. Tamura, MEGA7: Molecular Evolutionary Genetics Analysis Version 7.0 for Bigger Datasets. *Mol Biol Evol* **33**, 1870-1874 (2016).
9. F. Ronquist, J. P. Huelsenbeck, MrBayes 3: Bayesian phylogenetic inference under mixed models. *Bioinformatics* **19**, 1572-1574 (2003).
10. M. A. Suchard *et al.*, Bayesian phylogenetic and phylodynamic data integration using BEAST 1.10. *Virus Evol* **4**, vey016 (2018).
11. B. F. de Carvalho Dominguez Souza *et al.*, A novel hepatitis B virus species discovered in capuchin monkeys sheds new light on the evolution of primate hepadnaviruses. *J Hepatol* 10.1016/j.jhep.2018.01.029 (2018).
12. B. Muhlemann *et al.*, Ancient hepatitis B viruses from the Bronze Age to the Medieval period. *Nature* **557**, 418-423 (2018).
13. A. Rasche, A. L. Sander, V. M. Corman, J. F. Drexler, Evolutionary biology of human hepatitis viruses. *J Hepatol* **70**, 501-520 (2019).
14. N. M. Foley, M. S. Springer, E. C. Teeling, Mammal madness: is the mammal tree of life not yet resolved? *Philos Trans R Soc Lond B Biol Sci* **371** (2016).
15. L. Orlando *et al.*, Recalibrating Equus evolution using the genome sequence of an early Middle Pleistocene horse. *Nature* **499**, 74-78 (2013).
16. J. T. Vilstrup *et al.*, Mitochondrial phylogenomics of modern and ancient equids. *PLoS One* **8**, e55950 (2013).
17. S. Rossel *et al.*, Domestication of the donkey: timing, processes, and indicators. *Proc Natl Acad Sci U S A* **105**, 3715-3720 (2008).
18. J. Bough, *Donkey* (Reaktion Books, 2012).
19. G. Baele, P. Lemey, S. Vansteelandt, Make the most of your samples: Bayes factor estimators for high-dimensional models of sequence evolution. *BMC Bioinformatics* **14**, 85 (2013).
20. P. Simmonds, SSE: a nucleotide and amino acid sequence analysis platform. *BMC Res Notes* **5**, 50 (2012).
21. K. S. Lole *et al.*, Full-length human immunodeficiency virus type 1 genomes from subtype C-infected seroconverters in India, with evidence of intersubtype recombination. *J Virol* **73**, 152-160 (1999).
22. A. E. Durham, K. C. Smith, J. R. Newton, An evaluation of diagnostic data in comparison to the results of liver biopsies in mature horses. *Equine Vet J* **35**, 554-559 (2003).
23. N. D. Theise, Liver biopsy assessment in chronic viral hepatitis: a personal, practical approach. *Mod Pathol* **20 Suppl 1**, S3-14 (2007).

24. L. C. Junqueira, G. Bignolas, R. R. Brentani, Picrosirius staining plus polarization microscopy, a specific method for collagen detection in tissue sections. *Histochem J* **11**, 447-455 (1979).
25. Z. D. Goodman, Grading and staging systems for inflammation and fibrosis in chronic liver diseases. *J Hepatol* **47**, 598-607 (2007).